Improving detection of the melting layer using dual-polarization radar, NWP model data, and object identification techniques.

John Krause, CIMMS/University of Oklahoma, Norman, OK; and V. Lakshmanan, University of Oklahoma, Norman OK; and A. Ryzhkov, CIMMS/University of Oklahoma, Norman, OK.

Introduction:

An advanced version of the Melting Layer Detection Algorithm (MLDA) has been developed that can identify the areas affected by the impact of the melting layer at any given PPI. This new algorithm combines polarimetric radar data and NWP model information to properly designate the melting layer (or wet snow) and contamination from the melting layer in the storms with complex temperature profiles. The MLDA module is a key element of the Hydrometeor Classification Algorithm (HCA) and Quantitative Precipitation Estimation (QPE) algorithm employed on the polarimetrically upgraded network of the WSR-88D radars. The appropriate designation of the melting layer is crucial for distinguishing between the areas of pure rain, snow , and mixed-phase precipitation where different radar rainfall relations should be utilized.

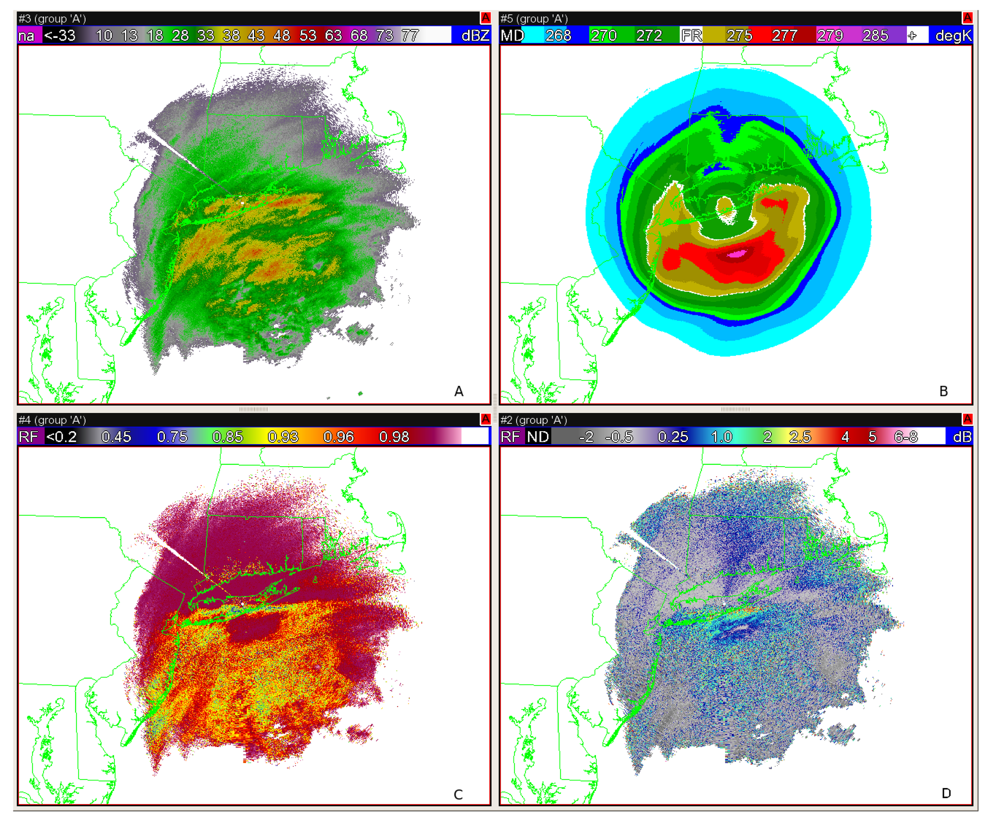

Fig 2. KOKX PPI images of A) Z, B) Temperature, C) ρ_{hv} and D) Z_{DR} on Feb 8th, 2013 at a 0.5° elevation

Motivation:

The existing version of the MLDA uses radar information at relatively high antenna elevations (between 4 and 10°) and the ML designation is projected onto lower elevations assuming that the precipitation field is relatively uniform in the horizontal direction (Giangrande et al. 2008). The assumption of the horizontal uniformity does not hold in the presence of frontal boundaries. Additionally, the performance of the existing MLDA may be compromised in intense cold-season storms, which are characterized by low and rapidly changing melting layers, and/or spatially complex melting layers. Furthermore, the existing MLDA can be confused by radar signatures from biota and may be unable to designate the height of the melting layer (ML) if there are no precipitation data near the radar (i.e., in the cone between elevations 4 and 10°).

The modified version of MLDA provides ML designation at all antenna elevations without the need to assume horizontal uniformity. The wet bulb temperature information retrieved from the NWP models is utilized to constrain the radar-based designation and to delineate the areas of "true" ML (or wet snow) as opposed to the regions of the "ML contamination" identified from the radar data. Due to the effects of radar beam broadening with distance, the areas of the ML contamination are usually wider than the regions of "true" ML at lower elevations.

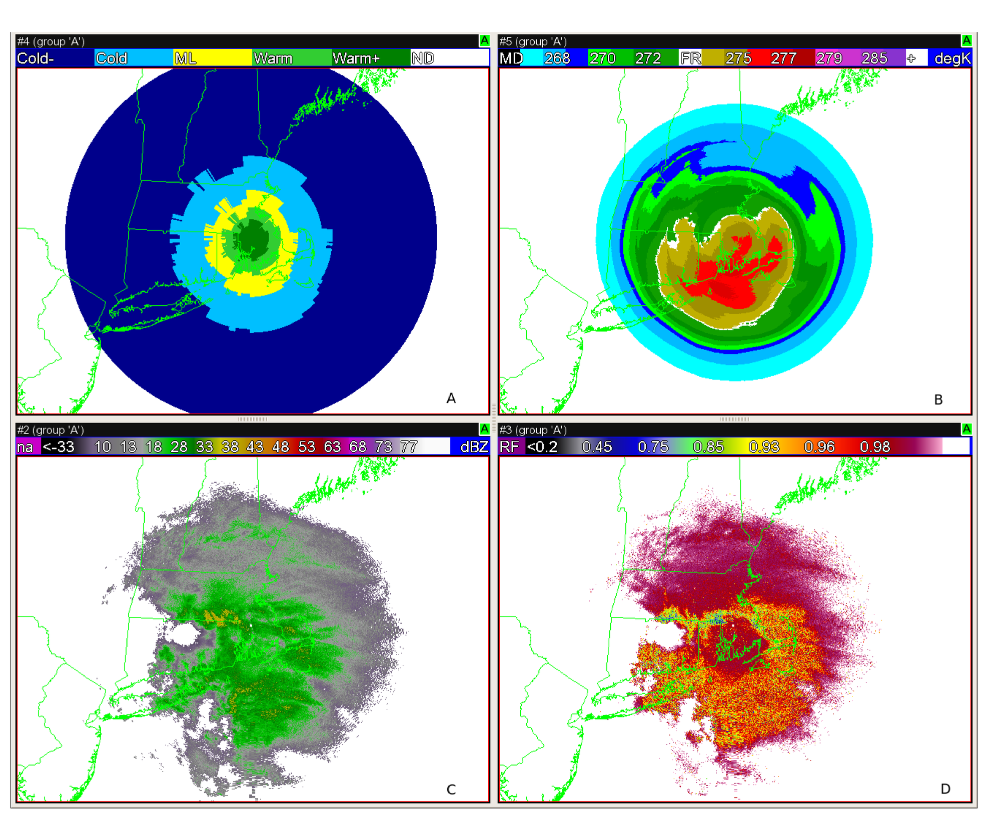

Fig. 1. KBOX PPI images of A) current MLDA, B) Temperature, C) Z, and D) ρ_{hv} on Jan 12th, 2012 at a 0.5° elevation

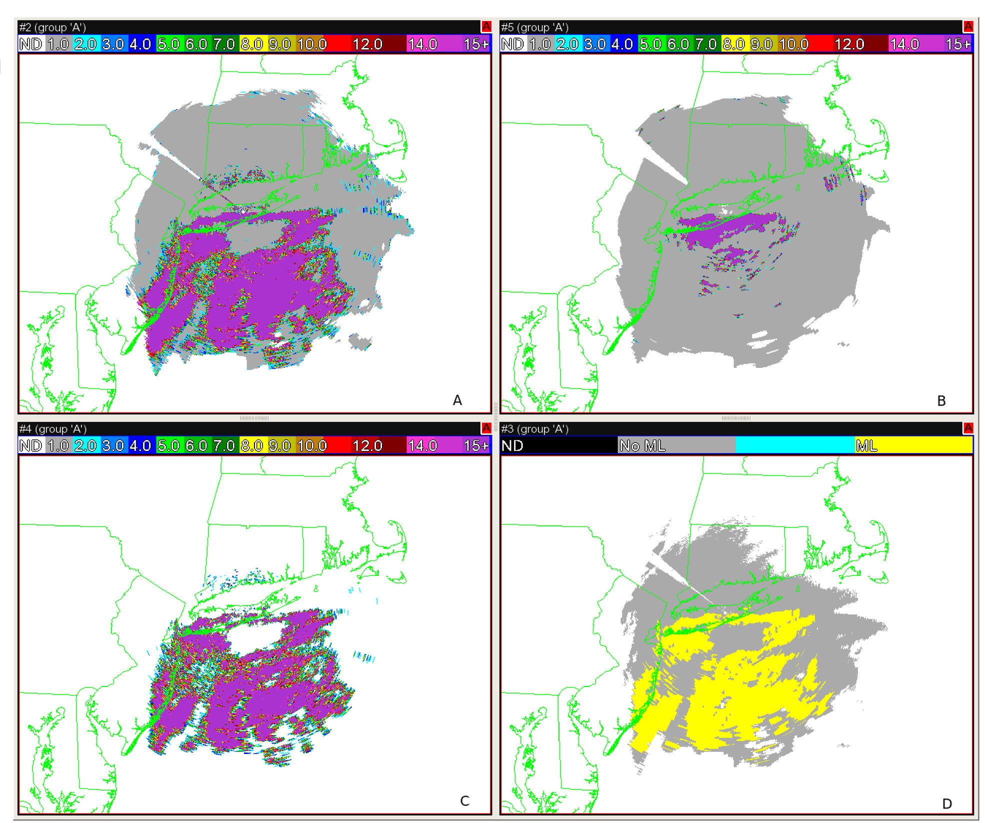

Fig. 3. KOKX PPI images of A) The ρ_{hv} interest field, B) The median Z_{DR} interest field, C) The wet snow interest field, and D) The combined melting layer interest field on Feb 8th, 2013 at a 0.5° elevation.

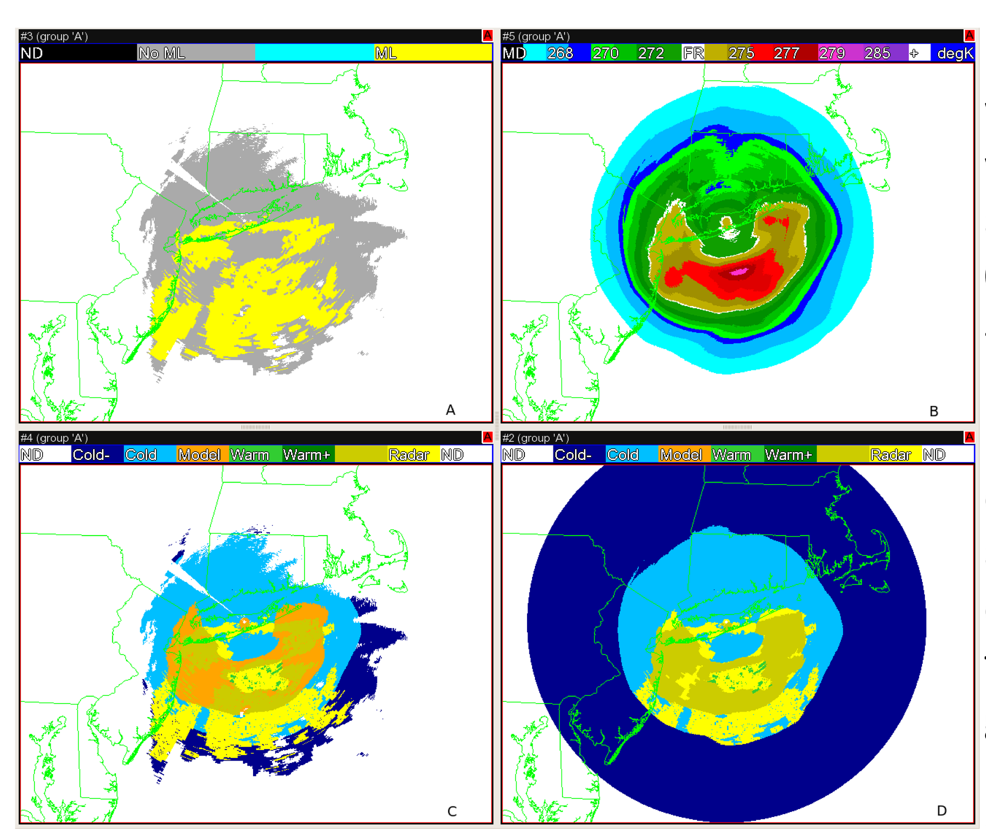

Fig. 4. KOKX PPI images of A) The radar determined ML, B) The wet bulb temperature, C)The combined radar and model data, and D) The final MLDA product on Feb 8th, 2013 at a 0.5° elevation.

Method:

A 2D median filter is applied to the Z_{DR} data at a given elevation. The filter determines the median Z_{DR} value from a 9 azimuth by 9 gate area. For the WSR-88D network this equates to a filter size of approximately 2kmx2km at a distance of 50km from the radar.

The median Z_{DR} values are then aggregated by counting the number of Z_{DR} observations that were greater than 0.8dB within a 25 gate 2D (5 azimuth x 5 gate) area. The number of observations greater than the threshold (0.8db) becomes an interest field for that variable, an integer that ranges in value from 0 to 25. (Fig 3b) A similar process is performed on ρ_{hv}. An interest field was created by counting the number of gates over a 2D area (5 azimuth x 5 gate)centered on the point that were less than 0.97. (Fig 3a)

Using the procedure from Giangrande et al. (2008), locations in the radar domain that fit the description of wet snow are identified. Note that in the existing MLDA such a procedure is utilized only at elevations between 4 and 10°. Then the interest field was computed by counting the number of wet snow detections over the 2D area as above. (Fig 3c)

All three density values are combined, equally weighted, into a final MLDA interest field using a simple summation. A threshold of 40 is used to identify the bins that contain data that are contaminated by melting hydrometeors. (Figs. 3d, 4a)

The wet bulb temperature T_w is computed from HRRR (High Resolution Rapid Refresh) model data and projected into the radar domain(Fig 4b). Model data are overlaid on the radar domain as follows. Locations with temperatures between 0 and 3°C are marked as ML (dark yellow if the radar detects a ML, orange if the radar does not), the areas where 3 < T_w < 8°C are colored green and considered warm, and areas with T_w > 8°C are considered very warm and colored dark green. Cold areas with T_w ranging from 0°C to -5°C are painted in blue and very cold areas with T_w < -5°C are shown in dark blue (Fig 4c).

Because pristine ice crystals often share many characteristics of melting layer contamination, model data are used to eliminate these false detections. ML contamination for radar gates whose model wet bulb temperature is less than -5°C are removed. Biota and ground clutter near the radar can look similar to melting layer contamination so ML contamination for the gates with a wet bulb temperature greater than 8°C were also removed (Fig 4d).

Giangrande, e.t. al., 2008: Automatic designation of the melting layer with a polarimetric prototype of the WSR-88D radar. *J. Appl. Meteor.*, **47**, 1354-1364.

Partial Funding for this research was provided under NOAA-OU Cooperative Agreement #NA17RJ1227.

Results:

Fig 5.

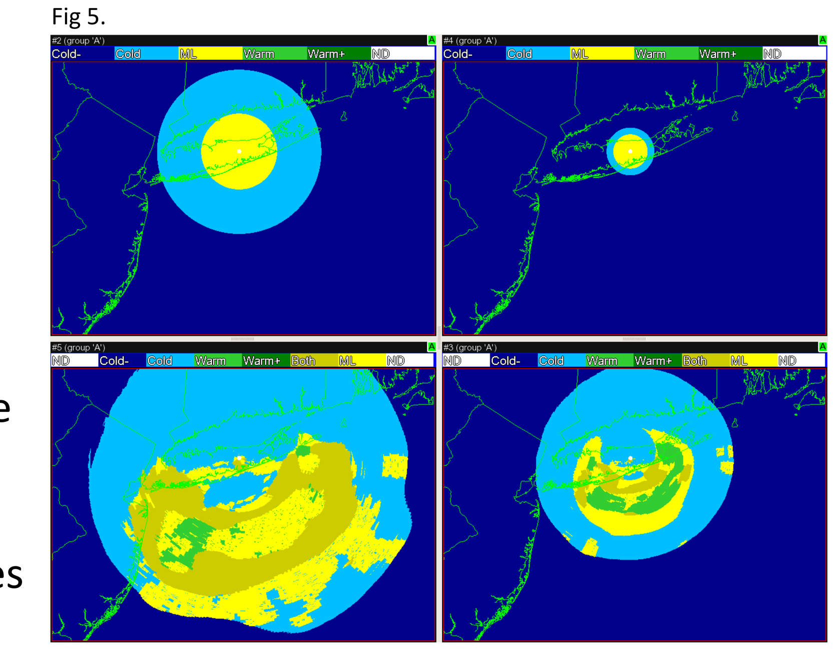

Fig 6.

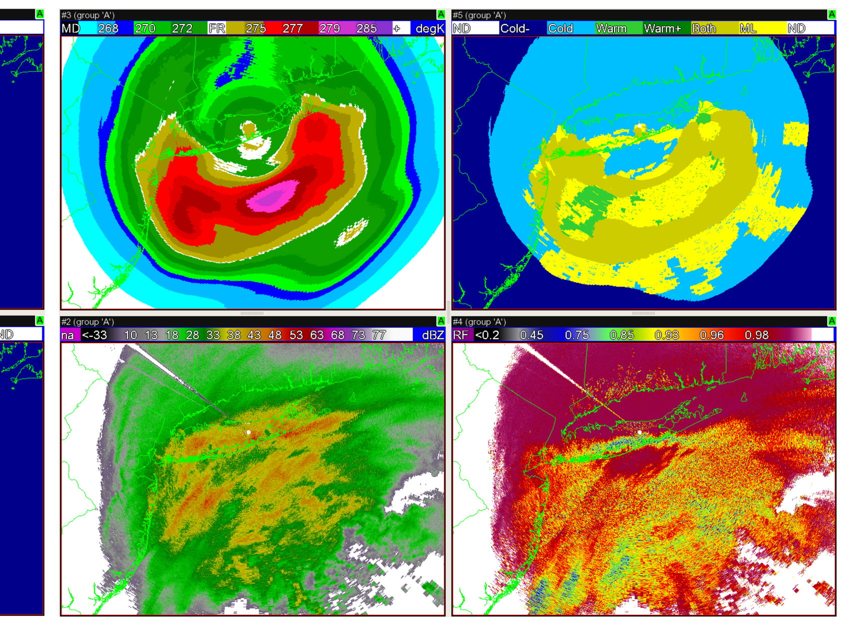

Fig 7.

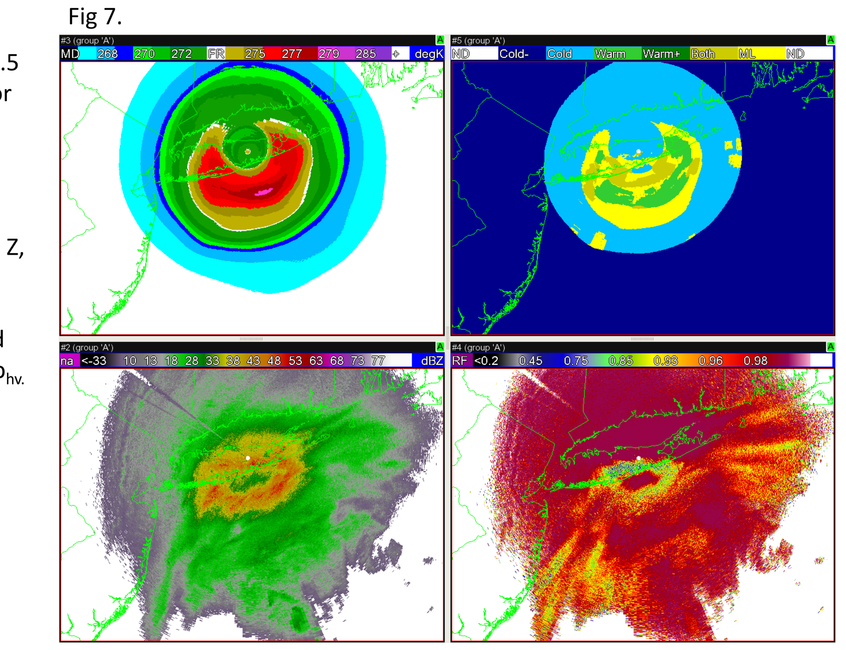

Fig 5. (upper left) KOKX PPI images of the current MLDA for 0.5 elevation, the current MLDA for 1.45 elevation, new MLDA for 0.5 elevation and new MLDA for 1.45 elevation on Feb 8th, 2013

Fig 6. (upper right) KOKX of PPI images all at 0.5 elevation, zoomed in to show detail. Wetbulb temperature, new MLDA, Z, and ρ_{hv}.

Fig 7. (right) KOKX of PPI images all at 1.45 elevation, zoomed in to show detail. Wetbulb temperature, new MLDA, Z, and ρ_{hv}.

The observations from the KOKX WSR-88D radar (above) on Feb 8th, 2013 and the KBOX WSR-88D radar (below) on Jan 12th, 2012 are good examples illustrating the complexity of the ML in winter storms. In both cases, a warm front is moving northward and a shallow region of warm air extends ahead of it aloft. The current MLDA method cannot capture the local spatial inhomogeneity of temperature and assumes that the melting layer detected south of the radar is present north of the radar which is far from reality. The new MLDA is able to discriminate between cold air and snow north of the radar and warmer air filled with mixed-phase hydrometeors to the south. Future goals for this project include testing and improving the algorithm with a diverse dataset and extending the algorithm to cover the entire WSR-88D network.

Fig 8.

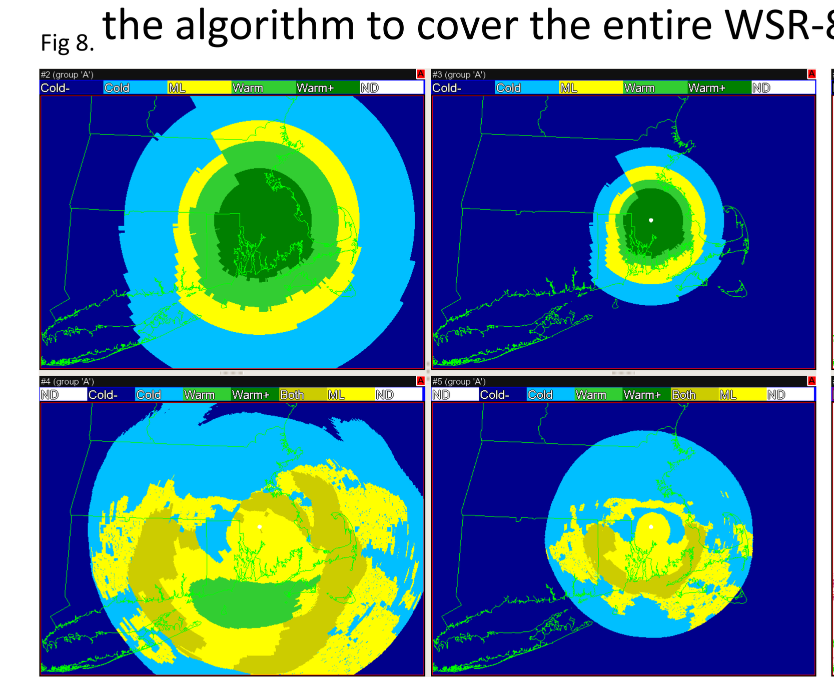

Fig 9.

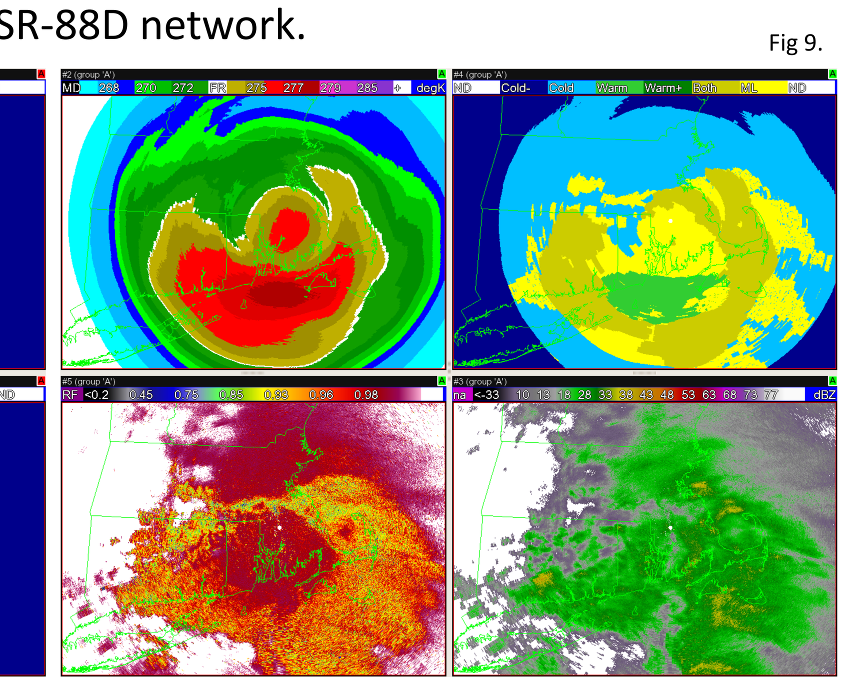

Fig 10.

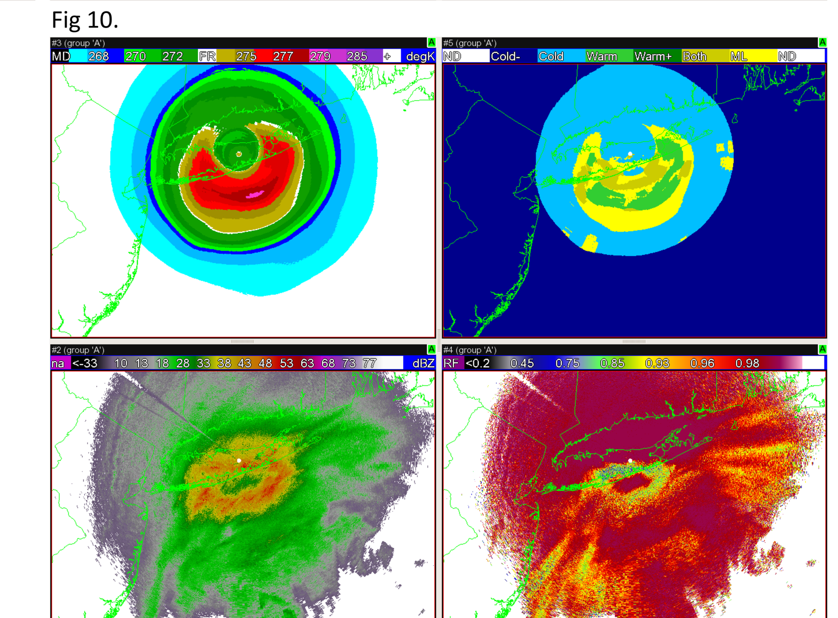

Fig 8. (upper left) KBOX PPI images of the current MLDA for 0.5 elevation, the current MLDA for 1.45 elevation, new MLDA for 0.5 elevation and new MLDA for 1.45 elevation on Jan 12th, 2012

Fig 9. (upper right) KBOX PPI images all at 0.5 elevation on Jan 12th, 2012: Wetbulb temperature, new MLDA, Z, and ρ_{hv}.

Fig 10. (right) KBOX PPI images all at 1.45 elevation on Jan 12th, 2012: Wetbulb temperature, new MLDA, Z, and ρ_{hv}.